Simulating Temperature Programmed Desorption of Water on Hydrated γ-Alumina from First-Principles Calculations

Jérôme Joubert, Paul Fleurat-Lessard, Françoise Delbecq,* and Philippe Sautet

Laboratoire de Chimie - UMR CNRS 5182, Ecole Normale Supérieure de Lyon, 46 Allée d'Italie, 69364 Lyon Cedex 07, France

Received: November 16, 2005; In Final Form: February 8, 2006

The knowledge of the properties of γ-alumina is of great importance in order to control its surface for numerous applications. We investigate the kinetic behavior of the hydrated alumina (110) surface toward water desorption: the minimum energy path is presented for successive desorption steps starting from the completely hydrated surface toward the dehydrated one. It appears that water desorption is a non activated process. A kinetic model is proposed based on an extension of the Eyring theory. This model is a useful tool to understand the evolution of water coverage during the pretreatment of alumina. It is then used to model temperature programmed desorption experiments for various heating rates. The shape of the desorption curve is qualitatively reproduced, and the differences between theory and experiments are discussed.

Introduction

γ-Alumina (Al_2O_3) is a key industrial material with numerous applications. It can be used as a catalyst or, more widely, as a catalyst support which enables dispersion of metal particles[1] or grafting of single-site organometallic complexes.[2] For all applications, the control of the surface nature and structure is fundamental. The hydration is of particular interest as it is in direct relation with the acidity of the surface and because it is present under usual experimental conditions. A pretreatment under various temperature conditions can be performed to control the water coverage, which can be evaluated by chemical reaction of hydroxyl groups with Grignard reagents or by ^1H NMR. The diversity of hydroxyl groups appears in infrared spectra. Digne et al. proposed an interpretation of infrared spectra based on DFT calculations.[3] This thermodynamic model links the surface hydroxyl coverage with the temperature of pretreatment of γ-alumina. An important further question is whether kinetic factors can affect this one-to-one relation between the coverage and the temperature of pretreatment.

In the present work, we investigate the kinetic behavior of hydrated alumina under temperature and pressure constraints on the basis of the determination of energy pathways for water desorption from hydrated γ-alumina model surfaces. We use the structural model developed by Digne et al. as a starting point for this purpose. For short desorption times, some structural differences exist between the metastable surface and its thermodynamic most probable state.

We use these kinetic results to model water temperature programmed desorption (TPD) experiments. The simple model that we use is an alternative to other methods that have been already proposed to simulate TPD.[4] To our knowledge, only one water TPD experiment on γ-alumina has been published.[5] The evaluation of the discrete distribution of adsoption energies of water on different surface sites has not been investigated using this experiment. Thus, we propose a simulation of water TPD experiments on γ-alumina for various heating rates to reveal the kinetic and thermodynamic behavior of water desorption.

Computational Methods

The calculations were performed in the framework of density functional theory (DFT) using a periodic description of the system as implemented in the VASP code.[6] The generalized gradient approximation was used in the formulation of Perdew and Wang PW91.[7] Atomic cores were described with the projected augmented wave method[8] (PAW), which is equivalent to an all electrons frozen core approach. The wave functions are developed on a basis set of plane waves. With the selected PAW potentials, a cutoff energy of 275 eV was adequate and yielded a converged total energy. Brillouin zone integration was converged with a 331 k-point mesh generated by the Monkhorst−Pack algorithm.[9] Minimum energy pathways have been found using the nudged elastic band (NEB) method with eight equally spaced images along the pathway.[10]

Energetic Pathways for Water Desorption. On a thermodynamic point of view, for $T = 300$ K and a partial water pressure $P_w = 31$ mbar (the average water partial pressure in the atmosphere for $T = 300$ K), the alumina surface is fully hydrated. As a result, we study the desorption from this fully hydrated surface. We concentrated on the (110) surface as the alumina crystallites expose between 70% and 83% of this type of facet. For this purpose, we used the model developed by Digne et al. which is based on a face-centered cubic lattice of oxygen atoms with a distribution of 25% of tetrahedral and 75% of octahedral aluminum atoms. A periodic slab with four layers of Al_2O_3 allows a correct description of the chemistry on the surface. The fully hydrated surface shows six water molecules per unit cell (that may be dissociated as hydroxyl groups). This system is indicated as **s6**. Similarly, the structures corresponding to a water coverage of N water molecules per unit cell will be indicated as **sN**. The structures corresponding to different water coverage have already been published, and the interested reader is directed to reference 3. The minimum energy path for the successive water desorption steps has been obtained from a

* Corresponding author. E-mail: francoise.delbecq@ens-lyon.fr.

10.1021/jp056633n CCC: $33.50 © 2006 American Chemical Society
Published on Web 03/11/2006

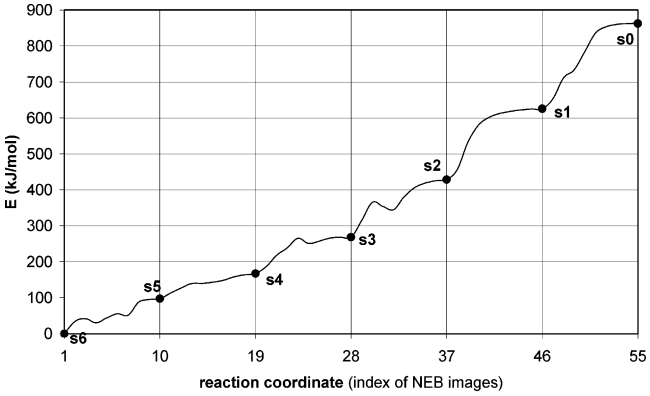

Figure 1. Minimum energy path for successive water desorption steps from a fully hydrated γ-Al_2O_3 (110) surface. See text for a discussion on the shape of the path.

TABLE 1: Desorption Energies along the Minimum Energy Pathway[a]

desorption reaction	$E_{\text{desorption}}$ (kJ mol^{-1})
s6 → **s5**	97
s5 → **s4**	70
s4 → **s3**	101
s3 → **s2**	160
s2 → **s1**	197
s1 → **s0**	237

[a] These values can differ slightly from those obtained by Digne et al. due to minor differences in the calculation methods.

SCHEME 1: Surface Rearrangement Prior to Desorption of a Water Molecule from s3 to s2

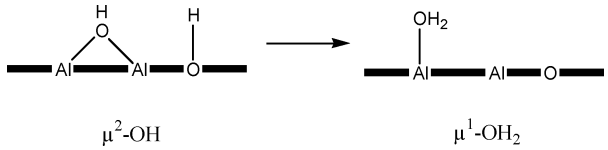

μ^2-OH μ^1-OH_2

juxtaposition of the NEB images between **sN** and **sN-1** and is presented in Figure 1. The reaction coordinate in Figure 1 is just defined by the index of the NEB images. It can be related to the distance d between the water molecule and the surface once the formation of the water molecule from hydroxyl groups is achieved. As we are looking at a desorption process, special care must be taken to define the upper limit of the reaction coordinate. In this work, we have considered that the desorption was complete when the energy change due to an increase of d was less than 5 kJ mol^{-1}.

The desorption energies are listed in Table 1. The expected trend would be an increase of the desorption energy with a decrease of coverage. This is not verified at high coverage due to contributions from hydrogen bonding: the desorption energy leading to **s5** is higher than the one leading to **s4** because the loss of energy in breaking hydrogen bonds is higher to form **s5** than it is to form **s4**, even if the strength of the Lewis site is similar. Due to these hydrogen bonds, the energy pathways show several minima between two consecutive **sN** surfaces for high coverage. These minima correspond to the departing water molecule interacting with hydroxyl groups. As the leaving water molecule in **s3** comes from a μ^2 hydroxyl group, the desorption occurs in two successive steps (see Scheme 1). First the water molecule is formed on the surface with a μ^1 coordination (minimum observed between **s3** and **s2)**. Then, the water molecule desorbs to give **s2**. After **s2**, no molecular minimum appears: this is due to the fact that on one hand the Lewis acid site is stronger and on the other hand only a few hydrogen bonds can appear.

The maxima between two consecutive **sN** surfaces are always lower in energy than the following **sN** surface on the pathway. Some tests have been performed in which the various intermediates between the **sN** structures are included in the kinetic model. The proportion of these intermediates remains very low and does not change the kinetic behavior of the system. As a result, it can be considered that no activation barrier exists for the successive desorption reactions other than the endothermicity of the step. This answers one of our questions: the one-to-one relation between coverage and temperature of pretreatment is maintained and it obeys the thermodynamic rules already presented by Digne et al.[3]

Kinetic Description of the Water Desorption. To simulate a TPD experiment with various heating rates, we must explore the kinetic behavior of the system at a given temperature. We propose to use the Eyring theory to evaluate kinetic constants as written in eq 1.

$$k = \frac{k_B T}{h} \frac{Z^{\ddagger}}{Z_{\text{reactant}}} e^{-(\Delta E^{\ddagger}/RT)} \tag{1}$$

As the desorption reactions are non activated, we explain precisely how $Z^{\ddagger}$ is calculated: it has been assumed that "transition states" correspond to products of desorption with a constraint on the allowed volume for translation of the desorbed water molecule. As the translation perpendicular to the surface is the major part of the reaction coordinate when reaching the region of the products, it has been suppressed from the partition function for the translation of the water molecule. As a result, the quasi-desorbed water molecule in the "transition state" is allowed to move parallel to the surface in a restricted area that has been taken equal to the unit cell area. The partition functions for translation will be indicated as $Z_t^{\ddagger}$ and Z_t for the quasi-desorbed water molecule and the really desorbed water molecule, respectively.

Rotational contributions to the partition function (Z_r) for the quasi-desorbed water molecule have been taken equal to the ones for the really desorbed water molecule.

All vibrational contributions are supposed to cancel between reactant and product or between reactant and "transition state" or product and "transition state", except the Al−O stretching vibration corresponding to the reaction coordinate at the beginning of the desorption reaction, to be coherent with the existence of the k_BT/h term in "transition state" vibrational partition function, which is at the core of the Eyring theory. This stretching vibration is not associated with a significant phonon dispersion as it is very localized and independent from the similar vibration in the closest other cells. The corresponding vibration partition function of the adsorbed water molecule will be indicated as Z_v.

We identify the activation energy to the reaction energy for desorption E_N. For the reverse reaction (i.e., adsorption), the activation energy is zero.

The rate of disappearance r_N^D of a **sN** unit cell per area unit by a desorption reaction is given by eq 2. The rate of formation r_N^A of a **sN** unit cell per area unit by an adsorption reaction is given by eq 3. The term x_N is defined as the fraction of **sN** unit cell per area unit. The rotational constants of the water molecule are indicated as θ_{ri}, $i = 1, 2, 3$ and the Al−O stretching frequency is indicated as ν. The exponential term in the denominator of β_N is due to zero-point energy.

$$r_N^D = \frac{k_B T}{h} \underbrace{\frac{1-e^{\frac{-h\nu}{k_B T}}}{e^{\frac{-h\nu}{2k_B T}}}}_{1/Z_v} \underbrace{\left(\frac{1}{2}\sqrt{\frac{\pi T^3}{\theta_{r1}\theta_{r2}\theta_{r3}}}\right)}_{Z_r} \underbrace{\left(s\frac{m_{H_2O}k_B T}{2\pi\hbar^2}\right)}_{Z_t^\ddagger} e^{\frac{-E_N}{RT}} x_N = \beta_N(T) x_N \quad (2)$$

$$r_N^A = \frac{k_B T}{h} \underbrace{\frac{\overbrace{\left(s\frac{m_{H_2O}k_B T}{2\pi\hbar^2}\right)}^{Z_t^\ddagger}}{\left(V\left(\frac{m_{H_2O}k_B T}{2\pi\hbar^2}\right)^{\frac{3}{2}}\right)}}_{Z_t} \frac{PV}{k_B T} x_{N-1} = \alpha(T,P) x_{N-1} \quad (3)$$

The system of equations that describes the kinetic behavior is written in a matrix form in eq 4 (below).

This system can be solved analytically. As an example, the result for $T = 770$ K and $P = 0.0013$ Pa, parameters which correspond to a standard pretreatment of alumina under high vacuum, is shown in Figure 2.

At the beginning of the desorption process, there is a coexistence of **s6**, **s4**, and **s3** (Figure 2); **s5** remains in very small quantity due to the non monotonic order of the desorption energies. After $t = 10^{-10}$ s there is an alternation of formation/disappearance of the different **sN** surfaces successively to reach the thermodynamic structure **s0** which corresponds to the complete desorption of water for this very low pressure and quite high temperature.

The time scale is very short and non completely physical. It can be due to the simplified approach that is used to obtain the values of prefactors in kinetic constants: only relative prefactors are significant. The time scale is sensitive to the allowed surface in the translation partition function of the transition state. For example, if we divide this surface by one hundred, the time scale is one hundred times larger. However, the physics of the desorption is well described and we can treat this allowed surface as a parameter to fit experiments that, to the best of our knowledge, have not yet been published.

It is possible to cancel the effect of this parameter by simulating a TPD experiment for which we can vary the heating rate. A very high heating rate (even if it is non physical) adapts the time scale of TPD to the time scale of our kinetic model of desorption. Of course, if we could fit the allowed surface on kinetic experiment, we would be able to use the actual heating rate. Here additional experimental data are required.

Temperature Programmed Desorption (TPD) of Water. Usual TPD experiments are associated with a continuous increase of the temperature and with a constant heating rate. For calculation convenience, TPD of water has been simulated by using the previous kinetic model during plateaus of temperature of various durations τ (for different heating rates), the proportions of different surface type **sN** at the end of a plateau being used as initial conditions for the next one. The difference of temperature between two plateaus is 1 K.[12] The results are reported in Figure 3.

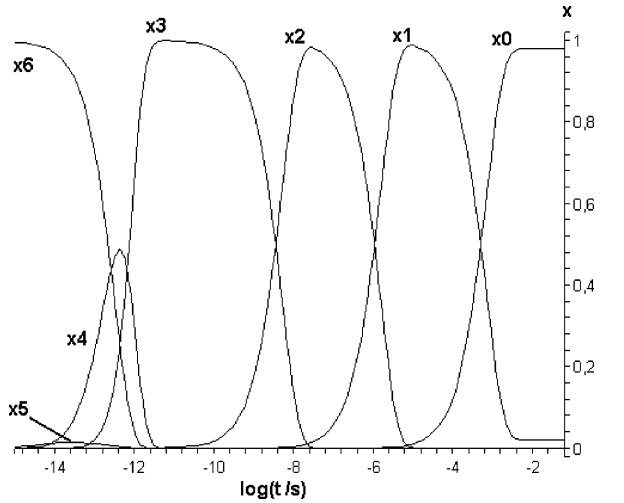

Figure 2. Composition x_N of the surface versus time. Simulation for $T = 770$ K and $P = 0.0013$ Pa (high vacuum 10^{-5} Torr). See text for comment on time scale.

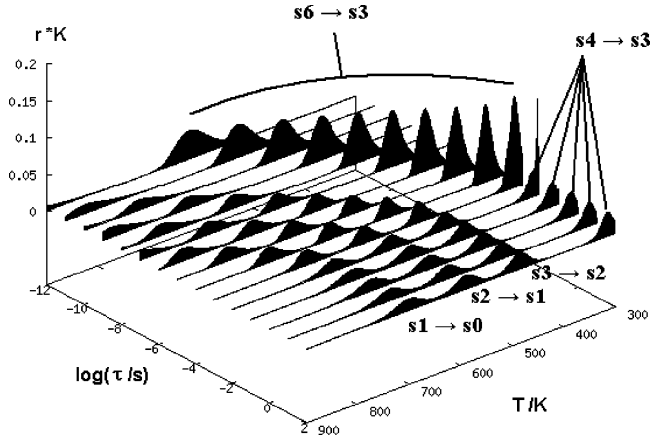

Figure 3. Model of TPD of water on a (110) surface of γ-Al_2O_3 for various duration τ of temperature plateaus: r, rate of water desorption (number of molecules desorbed per temperature unit).

For low heating rate (large values of τ), a thermodynamic equilibrium can be obtained during a plateau: the TPD spectrum remains unchanged for τ between 10^2 s and 10^{-2} s. For these values of the heating rate (10^{-2} to 10^2 K s^{-1}), the immediate desorption of two water molecules at $T = 300$ K leads to a large desorption peak ($r \approx 3$ K^{-1}) that has been omitted for the sake of clarity. This peak has been partly reported for $\tau = 10^{-2}$ s, which is the limit in order to achieve thermodynamic equilibrium: for faster heating rates not all the molecules have the time to desorb, some remain on the surface and desorb at higher temperature. All the spectra present a peak structure which is the image of the discrete structure of the model surface, with distinct adsorption energies on different sites. This structure is shifted to higher temperature in the case of small τ values (high heating rates).

We can wonder whether the large peak corresponding to the immediate desorption of water molecules at low temperature

$$\frac{d}{dt}\begin{bmatrix} x_0 \\ x_1 \\ x_2 \\ x_3 \\ x_4 \\ x_5 \\ x_6 \end{bmatrix} = \begin{bmatrix} -\alpha & \beta_1 & 0 & 0 & 0 & 0 & 0 \\ \alpha & -\alpha-\beta_1 & \beta_2 & 0 & 0 & 0 & 0 \\ 0 & \alpha & -\alpha-\beta_2 & \beta_3 & 0 & 0 & 0 \\ 0 & 0 & \alpha & -\alpha-\beta_3 & \beta_4 & 0 & 0 \\ 0 & 0 & 0 & \alpha & -\alpha-\beta_4 & \beta_5 & 0 \\ 0 & 0 & 0 & 0 & \alpha & -\alpha-\beta_5 & \beta_6 \\ 0 & 0 & 0 & 0 & 0 & \alpha & -\alpha-\beta_6 \end{bmatrix} \begin{bmatrix} x_0 \\ x_1 \\ x_2 \\ x_3 \\ x_4 \\ x_5 \\ x_6 \end{bmatrix} \quad (4)$$

would be seen in an experiment. These molecules should desorb during an initiation period when the gas flow starts and decreases the water partial pressure before the beginning of the measurement. The actual surface that would be explored by TPD would be in fact a partially hydrated surface resulting from the decrease of water partial pressure from the atmospheric value to the one of the experiment.

When τ decreases, the peaks are delayed and broadened. For low values of τ (high heating rate), the first peak (low temperature) corresponds to the desorption of three water molecules simultaneously. At the end of the temperature program ($T = 900$ K), some water molecules remain on the surface.

The comparison between experimental TPD and this simulation is somewhat difficult because of the discrete adsorption energies. The experimental spectrum does not show several peaks[5] as there may be an approximately continuous distribution of adsorption energies linked to a higher heterogeneity of surface sites than in our simple model. Nevertheless, some trends are well reproduced: for intermediate τ, there is a large peak, higher than all the others for T between 300 and 400 K. Subsequent peaks with smaller rates of desorption can be associated with the tail of the experimental TPD spectrum.

The non continuous desorption being due to a lack of intermediate energy levels allowed for the system, some tests have been performed including intermediate states between the **sN** ones along the reaction coordinate and counting a desorption only when a **sN** structure is reached. This enlarges the peaks a little but does not significantly change the results: the continuous desorption experimentally observed cannot be obtained with model unit cells as small as the ones we used. Of course, our model cannot reproduce border effects on hydrated zones that are known to exist on the surface.[11] This zone structure can lead to a continuous distribution of desorption energies but cannot be represented by a periodic model.

Conclusion

In this article, we have used the transition state theory to study the kinetics of water desorption from γ-Al_2O_3. The exploration of the potential energy surface of hydrated γ-Al_2O_3 along the water desorption reaction coordinate is very instructive for the comprehension of the phenomena occurring during temperature pretreatment of alumina. We can conclude from the calculations that water desorption is a non activated reaction independent from the state of the water molecule prior to desorption (dissociated or not, on a tetrahedral or octahedral aluminum). This gives a more general value to the previous "static" thermodynamic study.

The knowledge of the potential energy surface is a starting point for a kinetic study of water desorption and allows us to describe the kinetic behavior of the system with only one parameter to be adjusted with experimental data.

TPD modeling in non thermodynamic conditions has been performed on the basis of the kinetic model. Such experiments in non thermodynamic conditions have unfortunately never been published but should be of great interest to validate the model and to bring new insight on the dynamic behavior of hydrated alumina.

Acknowledgment. The authors thank Vincent Krakoviack for useful discussions and the Centre Informatique National de l'Enseignement Supérieur (CINES) at Montpellier for CPU time.

References and Notes

(1) (a) Ertl, G.; Knözinger, H.; Weitkamp, J. *The Handbook of Heterogeneous Catalysis*, Wiley-VCH: Weinheim, 1997. (b) Euzen, P.; Raybaud, P.; Krokidis, X.; Toulhoat, H.; Le Loarer, J. L.; Jolivet, J. P.; Froidefond, C. in *Handbook of Porous Materials*; Schüth, F., Sing, K., Weitkamp, J., Eds.; Wiley-VCH: Weinheim, 2002.

(2) (a) Jezequel, M.; Dufaud, V.; Ruiz-Garcia, M. J.; Carrillo-Hermosilla, F.; Neugebauer, U.; Niccolai, G. P.; Lefebvre, F.; Bayard, F.; Corker, J.; Fiddy, S.; Evans, J.; Broyer, J. P.; Malinge, J.; Basset, J. M. *J. Am. Chem. Soc.* **2001**, *123*, 3520. (b) Nedez, C.; Lefebvre, F.; Choplin, A.; Niccolai, G. P.; Basset, J. M.; Benazzi, E. *J. Am. Chem. Soc.* **1994**, *116*, 8638.

(3) (a) Digne, M.; Sautet, P.; Raybaud, P.; Euzen, P.; Toulhoat, H. *J. Catal.* **2004**, *226*, 54. (b) Digne, M.; Sautet, P.; Raybaud, P.; Euzen, P.; Toulhoat, H. *J. Catal.* **2002**, *211*, 1.

(4) Hansen, E. W.; Neurock, M. *Surf. Sci.* **2000**, *464*, 91.

(5) Men, Y.; Gnaser, H.; Ziegler, C. *Anal. Bioanal. Chem.* **2003**, *375*, 912.

(6) (a) Kresse, G.; Furthmüller, J. *Comput. Mater. Sci.* **1996**, *6*, 15. (b) Kresse, G.; Furthmüller, J. *Phys. Rev. B* **1996**, *54*, 11961.

(7) Perdew, J. P.; Chevary, J. A.; Voslo, S. H; Jackson, K. A.; Pederson, M. R.; Singh, D. J. Fiolhais, C. *Phys. Rev. B* **1992**, *46*, 6671.

(8) (a) Blöchl, P. E.; Först, C. J.; Schimpl, J. *Bull. Mater. Sci.* **2003**, *26*, 33. (b) Blöchl, P. E. *Phys. Rev. B* **1994**, *50*, 17953.

(9) Monkhorst, H. J.; Pack, J. D. *Phys. Rev. B 13* **1976**, 5188.

(10) Jónsson, H.; Mills, G.; Jacobsen, K. W. in *Classical and Quantum Dynamics in Condensed Phase Simulations*; Berne, B. J., Ciccotti, G., Coker, D. F., Eds.; World Scientific: Singapore, 1998; p 385.

(11) Métivier, R.; Leray, I.; Roy-Auberger, M.; Zanier-Szydlowski, N.; Valeur, B. *New J. Chem.* **2002**, *26*, 411.

(12) For a constant heating rate, it is possible to use shorter plateaus with a smaller difference of temperature between two plateaus. Some tests have been performed with a difference of 0.1 K and a duration of the plateaus divided by ten: this does not affect the results.